

Available online at www.sciencedirect.com

ScienceDirect

journal homepage: www.elsevier.com/locate/radcr

Case Report

Human T-cell lymphotropic virus type 1 (HTLV-1)-associated bronchioloalveolar disorder required differentiation from fibrotic chronic hypersensitivity pneumonitis [☆]

Tomonori Chikasue, MD^{a,*}, Akiko Sumi, MD, PhD^a, Shuichi Tanoue, MD, PhD^a, Toshi Abe, MD, PhD^a, Masaki Tominaga, MD, PhD^b, Junya Fukuoka, MD, PhD^c, Kiminori Fujimoto, MD, PhD^a

^a Department of Radiology, Kurume University School of Medicine, 67 Asahi-machi, Kurume, Fukuoka, 830-0011, Japan

^b Division of Respirology, Neurology, and Rheumatology, Department of Medicine, Kurume University School of Medicine, Kurume, Fukuoka, Japan

^c Department of Pathology, Nagasaki University Graduate School of Biomedical Sciences, Nagasaki, Japan

ARTICLE INFO

Article history:

Received 9 February 2022

Revised 26 March 2022

Accepted 30 March 2022

Keywords:

HTLV-1 (Human T-cell leukemia virus type 1)

HABA (HTLV-1-associated bronchioloalveolar disorder)

CHP (chronic hypersensitivity pneumonitis)

Fibrotic hypersensitivity pneumonitis

Thin-section CT

ABSTRACT

We encountered a case of HTLV-1-associated bronchioloalveolar disorder (HABA) that was difficult to distinguish from fibrotic chronic hypersensitivity pneumonitis (CHP). Chest thin-section computed tomography (CT) showed diffuse micronodules and revealed peribronchovascular and perilobular distribution. Further, thickening of the interlobular septa, areas of ground-glass attenuation, traction bronchiectasis/bronchiolectasis, and air trapping were observed. Based on these findings, diseases that cause lymphatic tract abnormalities and fibrotic CHP were considered differential diseases. A surgical lung biopsy was performed, and an HTLV-1 antibody was detected using the Western blot analysis of bronchoalveolar lavage fluid. The final diagnosis of HABA was made through a multidisciplinary discussion.

© 2022 The Authors. Published by Elsevier Inc. on behalf of University of Washington.

This is an open access article under the CC BY-NC-ND license

(<http://creativecommons.org/licenses/by-nc-nd/4.0/>)

[☆] Competing Interest: The authors declare no conflicts of interest associated with this manuscript.

* Corresponding author.

E-mail address: chikasue_tomonori@med.kurume-u.ac.jp (T. Chikasue).

<https://doi.org/10.1016/j.radcr.2022.03.108>

1930-0433/© 2022 The Authors. Published by Elsevier Inc. on behalf of University of Washington. This is an open access article under the CC BY-NC-ND license (<http://creativecommons.org/licenses/by-nc-nd/4.0/>)

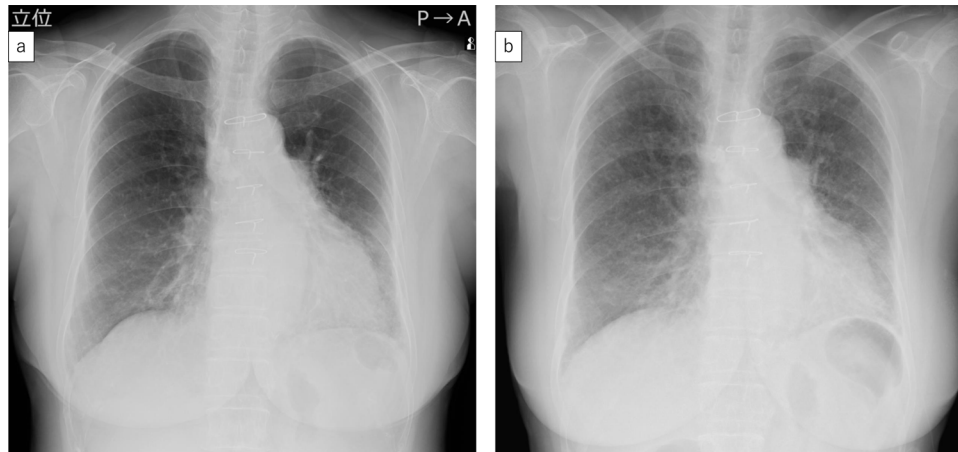


Fig. 1 – (A) Chest radiograph taken 13 years after coronary artery bypass surgery shows cardiac enlargement and slight ground-glass opacities in the bilateral lower lung fields. (B) Chest radiograph was taken 2 months after previous chest radiograph (A) presents ground-glass opacities expanded to the bilateral upper lung fields, and profuse micronodules appear diffusely. The severity of cardiac enlargement was unchanged.

Introduction

Human T-cell lymphotropic virus type 1 (HTLV-1) infection is endemic in tropical areas and southwestern Japan and has recently been reported in the United States and some European countries [1]. HTLV-1 is an etiological retrovirus of adult T-cell leukemia/lymphoma (ATLL) and is also associated with a nonmalignant neurological disorder known as HTLV-1-associated myelopathy (HAM) [2]. The lung is a preferential site for HTLV-1 infection. Pulmonary computed tomography (CT) findings in HTLV-1 carriers mainly demonstrate centrilobular nodules, ground-glass opacities, thickening of bronchovascular bundles, interlobular septal thickening, and bronchiectasis [3]. Presently, fibrotic chronic hypersensitivity pneumonitis (CHP) is a chronic inflammatory and fibrotic reaction caused by long-term exposure to inorganic antigens. This clinical entity can present centrilobular, reticular, and architectural distortions on high-resolution CT scans, which are often indistinguishable from those presented by other chronic interstitial lung diseases [4].

We herein report our experience with a case of HTLV-1-associated bronchioloalveolar disorder (HABA) that required differentiation from fibrotic CHP.

Case report

A 73-year-old Japanese woman without any smoking history had been followed up in the past 15 years under the suspicion of interstitial pneumonia. She had undergone coronary artery bypass grafting surgery in her 50s without any complications. Due to difficulties in breathing in late December 2017, she had visited a local doctor. As interstitial pneumonia was suspected on the chest radiograph, the patient was referred to the Center for Respiratory Diseases of our hospital in January 2018.

The patient had a respiratory rate of 20 breaths/min, a pulse rate of 86 beats/min, blood pressure of 102/60 mmHg,

and body temperature of 36.3°C. Transcutaneous oxygen saturation (SpO₂) in room air was low (93% at rest and 88% during ambulation). Chest auscultation revealed inspiratory fine crackles in both lungs with dominant lower lung fields. At this admission, the physical examination did not reveal Raynaud's phenomenon, eruptions or swelling of any joints, or dry eyes or mouth. Clubbed finger was not observed.

Laboratory data on admission showed a white blood cell count of 5400/ μ L. No abnormal cells were detected in the peripheral blood smear. The lactate dehydrogenase (LDH) level was 306 IU/L (within the normal range). High serum levels of C-reactive protein (1.17 [normal \leq 0.14] mg/dL) and soluble interleukin-2 receptor (1077 [normal 157-474] U/dL) were observed. In addition, each marker for interstitial lung diseases showed a high level as follows: sialylated carbohydrate antigen KL-6, 1297 (normal < 500) U/dL; surfactant protein D, 215 (normal < 110) ng/mL; and surfactant protein A, 74.7 (normal < 43.8) ng/mL.

Chest radiographs at this admission showed diffuse micronodules and ground glass opacities in the bilateral lungs (Fig. 1). Chest thin-section CT (Fig. 2) showed diffuse distributed micronodules, which were relatively hyperattenuated, well defined, and uniform in size (1-3 mm in diameter). The micronodules were diversely distributed, and some were located in the centrilobular area; however, they mainly showed peribronchovascular and perilobular distribution. Furthermore, the interlobular septal thickening, areas of ground-glass attenuation, and traction bronchiectasis/bronchiolectasis were predominantly seen in bilateral lower lobes. Air trapping, which was also predominantly observed in the lower lobes, exhibited a mosaic attenuation pattern (resembling the 3-density pattern) [5]. Based on these findings, we considered the diseases that caused lymphatic tract abnormalities, such as lymphoproliferative disorders, sarcoidosis, amyloidosis, HABA, collagen diseases, and drug-induced lung injury.

Additionally, fibrotic CHP was considered a differential disease due to the presence of centrilobular micronodular opac-

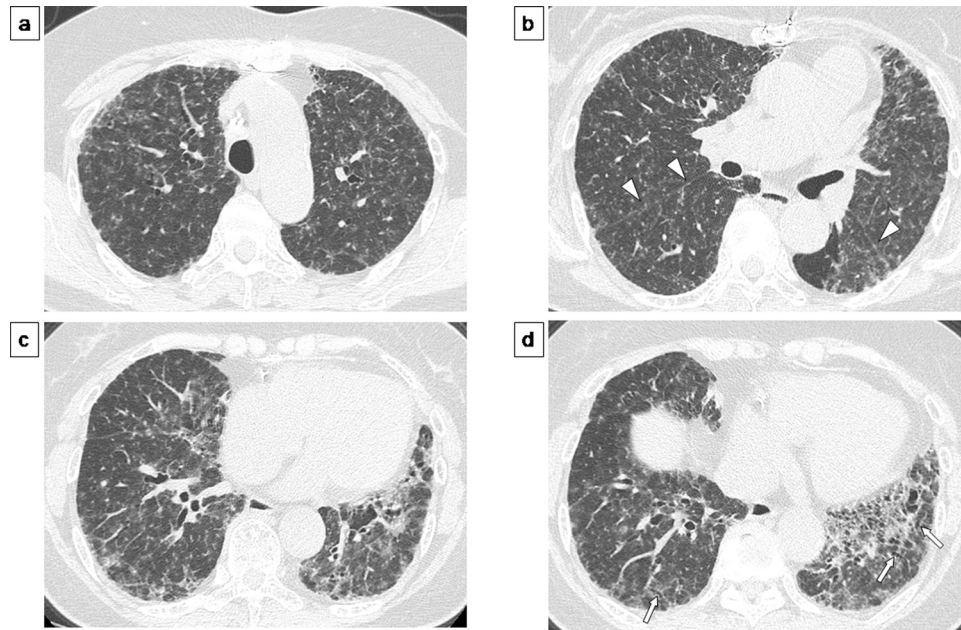


Fig. 2 – Chest CT scan (A-D) shows diffusely distributed micronodules, which were relatively hyperattenuated, well defined, and uniform in size (1-3 mm in diameter). The micronodules are diversely distributed and some are located in the centrilobular areas; however, they mainly showed peribronchovascular and perilobular distribution (arrowheads). Interlobular septal thickening, areas of ground-glass opacity, and traction bronchiectasis/bronchiolectasis are predominantly observed in bilateral lower lobes (arrow). Air trapping is also observed, especially in the lower lobes, and appears like a mosaic attenuation pattern (resembling the 3-density pattern). Metal artifacts are seen in the sternum from coronary artery bypass graft surgery.

ities in the upper lobes and air trapping in the lower lobes, suspected as an airway lesion [5].

A surgical lung biopsy was performed for a definitive diagnosis. Biopsy specimens from the right lower lobe (S8) showed that micronodules were located mainly around the airways, but sometimes in the periphery of the secondary lobule (Fig. 3A). These nodules consisted of severe lymphoid infiltration without atypia. These lymphocytes were predominantly T-cells on immunohistochemistry (CD3-positive cells were dominant and CD4/8 ratio was normal). Non-necrotizing granulomas and Langhans giant cells were also detected (Figs. 3B and C). Enlarged airspaces lined by bronchiolar-type epithelium were surrounded by dense fibrosis. Mucin and inflammatory cells filled most of the restructured airspaces (Fig. 3D).

The HTLV-1 antibody was detected using the Western blot analysis of bronchoalveolar lavage fluid (BALF) performed at a later date. No history of antigen inhalation or use of drugs that causes interstitial pneumonia was reported, and physical and laboratory findings suggestive of collagen disease were not found. According to the HP guidelines, both radiological and pathological diagnoses should “not be excluded” [5]. Therefore, the patient was diagnosed with HABA through a multidisciplinary discussion.

Discussion

HTLV-1, which is prevalent in southwestern Japan and the Caribbean Basin [6], is etiologically associated with ATLL and

several chronic inflammatory diseases, including HAM, and tropical spastic paraparesis, HTLV-1-associated arthropathy, HTLV-1-associated uveitis, and HABA. Although the mechanism of HTLV-1 that causes lung lesions remains unclear, Yamasato et al. showed that the expression levels of pro-inflammatory cytokines and chemokines activated by the protein product of the HTLV-1 pX gene are extremely high in the BALF of patients with HTLV-1-associated bronchitis, suggesting the active role of the virus in this disease [7].

Regarding the imaging features of HABA, Okada et al. reported that CT findings in HTLV-1 carriers mainly consist of centrilobular nodules (97%), thickening of bronchovascular bundles (56%), ground-glass opacities (52%), and bronchiectasis (51%) [3]. Furthermore, other cases of HABA with UIP pattern [8] or mosaic perfusion [9] have been reported. Thus, the CT image findings of HABA widely varied.

In contrast, typical chest CT findings of CHP considered as a differential disease in the present study are indistinct centrilobular peribronchiolar nodular opacities, that is, micronodules of varying numbers [10]. When fibrosis develops, chest radiographs show a reticular pattern and honeycombing, which sometimes are more severe in the upper lobes than in the lower ones. Volume loss may occur, particularly in the upper lungs, and peribronchial thickening may be visible [11]. Tateishi et al. reported that in the CT findings of IPF and CHP, upper or middle lung predominance, extensive ground-glass abnormality, and profuse micronodules were observed more frequently as discordant findings in CHP-UIP than in IPF ($P = .007, .010, \text{ and } .001$, respectively). Furthermore, in the regression analysis, extensive nodules (odds ratio [OR] 13.34

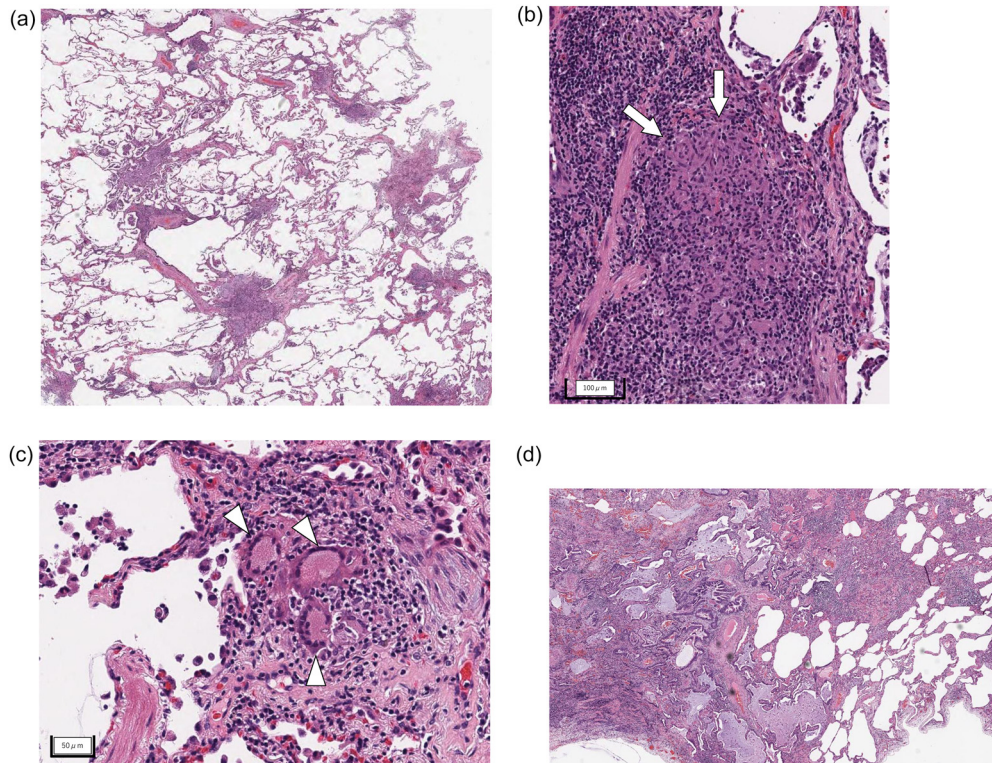


Fig. 3 – Biopsy specimen obtained from the right lower lobe (S8) shows that micronodules are mainly located around the airways, but sometimes in the periphery of the secondary lobule. (A, HE stain; X20) These nodules consist of severe lymphoid infiltration without atypia. These lymphocytes are predominantly T-cells on immunohistochemistry (CD3-positive cells dominant and normal CD4/8 ratio was). Non-necrotizing granulomas (arrows) and Langhans giant cells (arrowheads) are also detected (B, HE stain; X100, C, HE stain; X200). Enlarged airspaces are lined by bronchiolar-type epithelium and surrounded by dense fibrosis. Mucin and inflammatory cells fill many of the restructured airspaces (D, HE stain; X20).

(2.85–62.37)]; $P = .001$) and upper and middle lung predominance of findings [OR 2.86 (1.16–7.01); $P = .022$] remained as variables in the equation [12]. In addition, the diagnostic guideline for HP in adults was published in 2020, and CT patterns of HP are classified into 3 categories: typical, compatible, and indeterminate, depending on lesion distribution and the presence of small airway disease in non-fibrotic and fibrotic HP, respectively [5].

Furthermore, Okada et al. evaluated chest high-resolution CT scans in 553 patients with predominant centrilobular opacities or preferential centrilobular disease [13]. They histologically examined 2 types of centrilobular lesions: centrilobular nodules with a tree-in-bud appearance commonly found in HTLV-1 carriers and ill-defined centrilobular ground-glass nodules commonly found in HP. Pathologically, the tree-in-bud appearance represents lymphocytic infiltration distributed along respiratory bronchioles or bronchiolar luminal impaction with mucous or pus. On the contrary, ill-defined centrilobular ground-glass nodules pathologically represent peribronchiolar inflammation or deposition of hemorrhagic materials without plugging of small airways or dilated bronchioles.

Fukuoka, et al. reported pathological findings of HABA in 3 patients [14] who showed miliary micronodules randomly located in both lungs in the CT. Their histological features included lymphocytic infiltration distributed not only along the

respiratory bronchioles but also in the periphery of the secondary lobule.

In the thin-section CT images of this case, air trapping detected in the lower lobes appeared to be in a mosaic attenuation pattern and could be “compatible with HP” in the CT pattern of fibrotic HP according to the recently published guideline [5]. However, diffuse micronodules appeared to have a perilymphatic distribution, and the shape of micronodules was well defined, which was different from the ill-defined centrilobular ground-glass nodules observed in HP [13]. Furthermore, the histopathological findings in the present case showed severe lymphocytic infiltration in the perilymphatic areas as well as around the respiratory tract, which may be consistent with those of the previous report [14]. In addition, referring to the guidelines for hypersensitivity pneumonitis, no clear history of antigen exposure was available and the overall diagnosis, including the results of CT and pathological findings, was not excluded.

In conclusion, we experienced a case of HABA that required differentiation from fibrotic CHP. Thin-section CT showed that micronodules were well defined and perilymphatically distributed, which was consistent with HABA. However, lesions were also found in the upper lobes and were accompanied by ground-glass opacities and air trapping; therefore, CT alone would not have been able to completely rule out

CHP. In the absence of a clear history of antigen exposure, careful observation of CT findings, such as the distribution and nature of granular shadows, can assist in the diagnosis.

Patient consent

Written informed consent has been obtained from the patient.

REFERENCES

- [1] Watanabe T. Current status of HTLV-1 infection. *Int J Hematol* 2011;94:430–4. doi:[10.1007/s12185-011-0934-4](https://doi.org/10.1007/s12185-011-0934-4).
- [2] Sonoda S, Li HC, Tajima K. Ethnoepidemiology of HTLV-1 related diseases: ethnic determinants of HTLV-1 susceptibility and its worldwide dispersal. *Cancer Sci* 2011;102:295–301. doi:[10.1111/j.1349-7006.2010.01820.x](https://doi.org/10.1111/j.1349-7006.2010.01820.x).
- [3] Okada F, Ando Y, Yoshitake S, et al. Pulmonary CT findings in 320 carriers of human T-lymphotropic virus type 1. *Radiology* 2006;240:559–64. doi:[10.1148/radiol.2402050886](https://doi.org/10.1148/radiol.2402050886).
- [4] Silva CI, Churg A, Müller NL. Hypersensitivity pneumonitis: spectrum of high-resolution CT and pathologic findings. *AJR Am J Roentgenol* 2007;188:334–44. doi:[10.2214/AJR.05.1826](https://doi.org/10.2214/AJR.05.1826).
- [5] Raghu G, Remy-Jardin M, Ryerson CJ, et al. Diagnosis of hypersensitivity pneumonitis in adults. An official ATS/JRS/ALAT clinical practice guideline. *Am J Respir Crit Care Med* 2020;202:e36–69. doi:[10.1164/rccm.202005-2032ST](https://doi.org/10.1164/rccm.202005-2032ST).
- [6] Gibbs WN, Lofters WS, Campbell M, et al. Non-Hodgkin lymphoma in Jamaica and its relation to adult T-cell leukemia-lymphoma. *Ann Intern Med* 1987;106:361–8. doi:[10.7326/0003-4819-106-3-361](https://doi.org/10.7326/0003-4819-106-3-361).
- [7] Yamazato Y, Miyazato A, Kawakami K, Yara S, Kaneshima H, Saito A. High expression of p40(tax) and pro-inflammatory cytokines and chemokines in the lungs of human T-lymphotropic virus type 1-related bronchopulmonary disorders. *Chest* 2003;124:2283–92. doi:[10.1378/chest.124.6.2283](https://doi.org/10.1378/chest.124.6.2283).
- [8] Yamashiro T, Kamiya H, Miyara T, et al. CT scans of the chest in carriers of human T-cell lymphotropic virus type 1: presence of interstitial pneumonia. *Acad Radiol* 2012;19:952–7. doi:[10.1016/j.acra.2012.03.020](https://doi.org/10.1016/j.acra.2012.03.020).
- [9] Mikita K, Kobayashi H, Kanoh S, Ozeki Y, Motoyoshi K. A case of HTLV-1 associated bronchiolo-alveolar disorder showing progressive air trapping. *Nihon Kokyuki Gakkai Zasshi* 2008;46:1055–8 (in Japanese).
- [10] Buschman DL, Gamsu G, Waldron JA, Klein JS, King TE. Chronic hypersensitivity pneumonitis: use of CT in diagnosis. *AJR Am J Roentgenol* 1992;159:957–60. doi:[10.2214/ajr.159.5.1414806](https://doi.org/10.2214/ajr.159.5.1414806).
- [11] Adler BD, Padley SP, Müller NL, Remy-Jardin M, Remy J. Chronic hypersensitivity pneumonitis: high-resolution CT and radiographic features in 16 patients. *Radiology* 1992;185:91–5. doi:[10.1148/radiology.185.1.1523340](https://doi.org/10.1148/radiology.185.1.1523340).
- [12] Tateishi T, Johkoh T, Sakai F, et al. High-resolution CT features distinguishing usual interstitial pneumonia pattern in chronic hypersensitivity pneumonitis from those with idiopathic pulmonary fibrosis. *Jpn J Radiol* 2020;38:524–32. doi:[10.1007/s11604-020-00932-6](https://doi.org/10.1007/s11604-020-00932-6).
- [13] Okada F, Ando Y, Yoshitake S, et al. Clinical/pathologic correlations in 553 patients with primary centrilobular findings on high-resolution CT scan of the thorax. *Chest* 2007;132:1939–48. doi:[10.1378/chest.07-0482](https://doi.org/10.1378/chest.07-0482).
- [14] Fukuoka J, Tominaga M, Ichikado K, et al. Lung miliary micro-nodules in human T-cell leukemia virus type I carriers. *Pathol Int* 2013;63:108–12. doi:[10.1111/pin.12030](https://doi.org/10.1111/pin.12030).